Theoretical Study of Electronic Properties and Vibration Frequencies for Tri-Rings Layer (6, 0) Linear (Zigzag) SWCNT

Rehab Majed Kubba*, Khalida Aubead Samawi
Department of Chemistry, College of Science, University of Baghdad, Iraq , Baghdad , Iraq

Abstract.

DFT (3-21G, 6-31G and 6-311G/ B3LYP) and Semi-empirical PM3 methods were applied for calculating the vibration frequencies and absorption intensities for normal coordinates (3N-6) of the Tri-rings layer (6,0) Zigzag single wall carbon nanotube (SWCNT) at their equilibrium geometries which was found to have D_{6h} symmetry point group with C-C bond alternation in all tube rings.as well as mono ring layer. Assignments of the modes of vibration were done depending on the pictures of their modes applying by Gaussian 03 program. The whole relations for the vibration modes were also done including (CH stretching, νCC stretching, deformation in plane of the molecule (δCH, δring and δCCC), deformation out of plane of the molecule (γCH and γring (γCCC). Also include the assignment of puckering, breathing and clock-anticlockwise bending vibrations.

Comparison for the geometry (the relations for axial bonds, which are the vertical C-C bonds (linear bonds) in the rings layer and for circumferential bonds which are the outer ring bonds), electronic properties and IR active vibration frequencies (asymmetric modes) of (Mono and Tri) rings layer were done. Clear relationships were found in the results of an odd layer number (Mono and Tri-rings layer). The theoretical results allow a comparative view of the charge density at the carbon atoms too.

Keywords: Tri-rings layer Zigzag SWCNT, Electronic properties, Vibration frequencies.

دراسة نظرية للصفات الالكترونية ولترددات اهتزاز انبوب النانوكاربون نوع (6,0) زكزاك ثلاثي الطبقات

رحاب ماجد كبة، خالدة عبيد سماوي
كلية العلوم، قسم الكيمياء، جامعة بغداد، بغداد، العراق

الخلاصة

تضمن البحث استخدام إحدى طرق ميكانيك الكم التقريبية شبه التجريبية Semi-empirical method (parameter model 3 (PM3) وطريقة (DFT (6-311G,6-31G,3-21G/ B3LYP الأساسية غير التقريبية (لعناصر قاعدة متعددة) باستخدام برنامج Gaussian-03 في حساب الشكل الهندسي التوازني لانبوب النانوكاربون نوع زكزاك (6, 0) ثلاثي الطبقات الذي وجد امتلاكه للتماثل D_{6h}. و تم تصنيف ترددات اهتزاز طيف الأشعة تحت الحمراء وبعدد 3N-6 وتشخيصها تكافؤيا وتماثليا، وايجاد جميع العلاقات المتعلقة بالانماط المختلفة كترددات مط νCH و νCC و ترددات انحناء δCH وδCCC و γCH وγCC و γCCC،

*E:Rehab_mmr_kb@yahoo.com

المتضمنة الحركات التنفسية والانبعاجية. كذلك تمت دراسة بعض الصفات الفيزياوية كحرارة التكوين والطاقة الكلية وعزم ثنائي القطب والفرق الطافي ΔEHOMO-LUMO وتوزيع الكثافة الالكترونية-- الخ، عند الشكل الهندسي التوازني. تم التركيز في الدراسة على عناصر القاعدة الاكثر دقة في الحساب /6-311G) B3LYP)، وتمت مقارنة النتائج نظريا مع انبوب النانوكاربون نوع زكزاك (6, 0) احادي الطبقة. وكذالك تمت دراسة ومقارنة توزيع الكثافة الالكترونية على ذرات الكاربون.

Introduction

Carbon nanotubes (CNTs) have been intensively studied according their importance as a building block in nanotechnology. The special geometry and unique properties of carbon nanotubes offer great potential applications [1]. Various quantum mechanical studies were done for the physical properties of the nanotubes [2-6]. Structural deformation is expected to change their thermal and electronic properties too. The study of vibration of CNTs is for successful applications in nanotechnology. Specifically, some vibration modes of CNTs, e.g., radial breathing mode [7-10], beam-like bending mode, [11,12] and longitudinal mode [13], offers valuable probes for the molecular structures and the elastic properties of CNTs. On the other hand, CNTs consisting of straight concentric layers with circular cross-section could lose their structural symmetry due to the vibration in axial, circumferential and radial directions [14,15]. This could result in a sudden change in their physical properties (e.g., the electrical properties [16] and in turn, significantly affect their performance in nanostructures. Thus, similar to the buckling behavior [17] the vibration of CNTs turns out to be a major topic of great interest in nanomechanics, considerable efforts [18] have been devoted to capturing the fundamental vibration behaviors of CNTs by using experimental techniques [19] and multi-scale modeling tools [20-24]. Recently, the interest of the mechanics of CNTs has been transferred from their fundamental behavior to the effect of internal and external factors on the elastic properties [25-27], buckling [28-30] of CNTs. However no study could be found in the literature for a normal coordinate analysis of the simplest type of nanotube Tri rings-layer Zigzag SWCNT.

Methods of calculation

G03 program of Pople et al. [31] was applied throughout the present work.

Results and Discussion

In the recent study [32], the absorption intensities and assignment of the vibration frequencies of carbon nanotube were calculated for normal coordinates (3N-6) of [6] Zigzag single wall carbon nanotube. In this work the vibratory motions of Tri-rings layer (6,0) Zigzag single wall carbon nanotube (SWCNT) at their equilibrium geometrieswere calculated, define its geometric parameters, and distinguished between their axial (C-Ca) (vertical bonds) in the rings and circumferential (C-Cc) the outer ring bonds, both C-C bond alternation in all tube rings. figure-1, shows the two types of bonds of zigzag Tri ring layers CNT, a space filling, optimized geometry and repetitive sections of bonds due to its symmetry D_{6h}.Basic vibrations of SWCNTs were measured and assigned as breathing, puckering and clock-anti-clockwise deformation modes [7]. They were considered as finger print vibrations for the carbon nanotubes (CNTs) [8]. The active vibrations cause a change in its geometric structure. Measurements were done to study the impact of the puckering distortion on the electronic properties of CNTs [9-11].

For a normal mode of vibration to be infrared active, there must be a change in the dipole moment of the molecule during the course of vibration (during the vibrational motion of a molecule, a regular fluctuation in the dipole moment occurs, and a field is established which can interact with the electrical field associated with radiation). For the absorption of infrared radiation, a molecule must undergo a net change in its dipole moment as a result of its vibrational or rotational motions [12].

The classifications of carbon nanotube Tri-rings layer, determined by three numbers of ring layers, and the length of CNT, can also be described as single-walled nanotubes (SWNT), resembling by rolling a graphene sheet into a cylindrical structure are uniquely defined by specifying the coordinates of the smallest folding vector (n, 0) Zigzag SWCNT is composed of linear numbers of aromatic ring molecules. So the Tri-rings layer SWCNT is composed of linear six members of aromatic rings in each three layers. Its (PM3 and DFT (B3LYP/6-311G) calculated equilibrium geometry shows D_{6h} symmetry point group, as in figure-1.

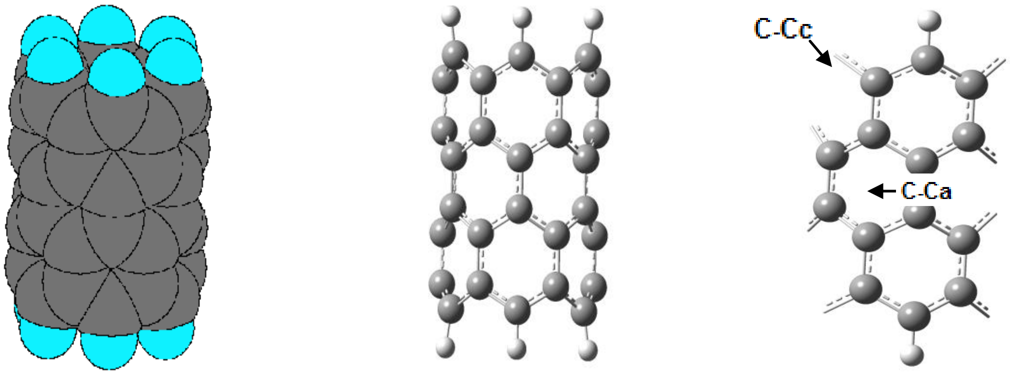

Space filling for tri-rings layer SWCNT **Tri-rings layer SWCNT (D_{6h})** **Repetitive section**

Figure 1- Space filling, equilibrium geometry and repetitive sections of bonds and angles for Tri-rings layer (6,0) Zigzag (SWCNT) according to their point group (D_{6h}).

Table-1 shows that for the Tri-rings layer SWCNT (C…Ca) bonds be shorter on going from outer rings layer to mid ring layer, the reverse was shown for the (C…Cc).The comparison of Mono-ring layer with Tri-rings layers, showed that the diameter decrease with increasing odd rings layer, the diameter of Mono ring layer (4.7370 Å) is lower than that for Tri-rings layers (4.8256 Å). The C-C bonds of the optimized Zigzag Tri-rings layer SWCNTs as well as for the optimized Zigzag Mono layer were all being conjugated double bonds. (C-H) and (C…Ca) bond length in Mono-ring layer was shorter than that inTri-rings layer, the reverse was found for (C…Cc) bond length, which decrease in length with increase in odd rings layer (Tri rings layers), and decrease in length on going from the outer rings layer to the mid ring layer**.**

Table 1- DFT (6-311G/ B3LYP) calculated bond distances for the calculated (Mono and Tri) rings layer (6,0) Zigzag SWCNT.

Odd layer Zigzag (SWCNT)	Diameter (Å)	Length (Å)	Bond length (Å)		
			C…Ca	**C…Cc**	**C—H**
***Mono-ring layer D_{6h}**	**4.7370**	**4.9722**	**1.4462**	**1.4133**	**1.0946**
Tri-rings layer D_{6h}	**4.8256**	**9.2647**	**1.4442 Outer 1.4362 Mid**	**1.4254 Outer 1.4341 Mid**	**1.0830**

C-Ca: axial bond.;C-Cc: circumferential bond [32].

The frontier molecular orbital's HOMO (the Highest Occupied Molecular Orbital) and LUMO (the Lowest Unoccupied Molecular Orbital), also have been calculated, as well as E_{HOMO}., E_{LUMO} represents the ability of the molecule to accept or donate electrons. The higher value of E_{HOMO} suggests the molecule donates electrons more probable, while the lower value of E_{LUMO} suggests the molecule accepts electrons more probable [33, 34].

Detailed result in table-2, showed that $\Delta H_{f,}$ and E_{HOMO}, increase with increasing number of odd rings layer, E_{LUMO}decrease with the increasing odd rings layer. $\Delta E_{HOMO\text{-}LUMO}$ decrease with increasing both, the number of odd and even rings layer.

Dipole moment μ is zero for two odd rings layer, Mono and Tri-rings layer because they have a center of inversion according to their symmetry D_{6h}.table-2, shows some physical properties of thecalculated (Mono and Tri)-rings layer (6, 0) Zigzag SWCNT at their equilibrium geometry.

Table 2- Some physical properties of the calculated (Mono and Tri) rings layer(6, 0) Zigzag SWCNT at their equilibrium geometry* **[32]**

Odd layer Zigzag (SWCNT)	m. wt. (g/ mol)	ΔH_f (kcal/mol)	μ (Debye)	$E_{tot.}$ (eV)	E_{HOMO} (eV)	E_{LUMO} (eV)	$\Delta E_{HOMO-LUMO}$ (eV)
Mono-ring* layer ($C_{24}H_{12}$)	300.359	353.370	0.000	-25071.916	-6.309	-2.586	3.723
Tri-rings layer ($C_{48}H_{12}$)	588.623	663.338	0.000	-49953.572	-5.670	-3.642	2.038

Figure-2, shows the frontier molecule orbital density distributions and energy levels of HOMO (Highest Occupied Molecular Orbital), and LUMO (the Lower Unoccupied Molecular Orbital) orbitals computed at the B3LYP/6-311G level for the Mono and Tri rings layer (6, 0) Zigzag SWCNT. As seen from figure-2, in HOMO and LUMO, electrons are mainly localized on the outer circumferential carbon atoms. The value of the energy separation between the HOMO and LUMO ($\Delta E_{HOMO-LUMO}$) is 2.038eV, for Tri rings layer less than for Mono ring layer 3.723eV and this lower energy gap indicates that the Tri rings layer is better for electrical conductivity.

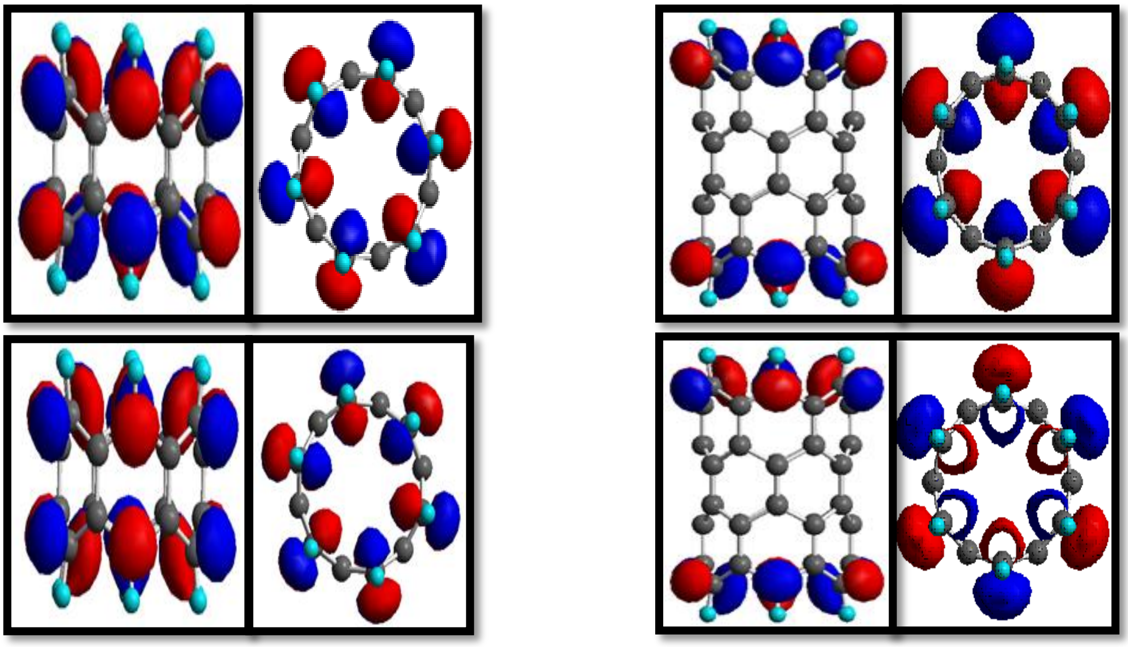

Homo **Homo**

(a) **(b)**

Figure 2-The frontier molecule orbital density distributions of: a) Mono ring layer (6, 0) Zigzag SWCNT, HOMO; LUMO (vertical and horizontal sections). b) Tri rings layer (6, 0) Zigzag SWCNT, HOMO; LUMO (vertical and horizontal sections).

Vibration frequency assignment of Tri-rings layer(6, 0) Zigzag SWCNT($C_{48}H_{12}$)

The Tri-rings layer Zigzag SWCNT posses 174 fundamental vibrations. Inspection of its irreducible representations, as defined by the symmetry character table, resulted in the following modes of vibration;

$\Gamma_{vibration} = \Gamma_{total} - (\Gamma_{rotation} + \Gamma_{translation}) = 3N-6 = 180 - 6 = 174 = 10A_{1g} + 4A_{2g} + 7B_{1u} + 8B_{2u} + 14E_{1u} + 15E_{2g} + 5A_{1u} + 9A_{2u} + 7B_{1g} + 8B_{2g} + 14E_{1g} + 15E_{2u}$

For SWCNTs, and relative to the (**б$_{+h}$**) reflection the vibration modes are classified as:

a- Symmetric modes with respect to б$_h$ (б$_{+h}$). These are out of plane (of the molecule).

Γб$_{+h}$ $= 10A_{1g} + 4A_{2g} + 15E_{2g} + 7B_{1u} + 8B_{2u} + 14E_{1u}$ **(In-plane modes of vibrations with respect to σ_h)= 87**

b- Antisymmetric modes with respect to $б_h$($б_{-h}$). These are in plane (of the molecule) modes of vibrations.

$Гб_{-h}$= $7B_{1g}$ + $8B_{2g}$+$14E_{1g}$ + $5A_{1u}$ + $9A_{2u}$ + $15E_{2u}$= 87

Symmetric modes with respect to $б_h$ ($б_{+h}$)

These are 68 modes of vibration in number, of which 40 are Raman active ($10A_{1g}$ **(polarized)** + $15E_{2g}$ **(depolarized)**), and 28 IR active ($14E_{1u}$).

νCH stretching vibrations

The frequency values range from (3029-3041cm^{-1}), showing the following correlations:

ν_{sym} CH str.(3041 cm^{-1}) (A_{1g}) ≅ ν_{asym}CH str. (3041 cm^{-1}) (A_{2u})

The highest IR absorption intensity is 55.779km/mol due to ν_{93}(3041 cm^{-1}) (A_{2u}).

ν(C--C stretching) vibrations

The calculated CC stretching vibration frequencies range from (1054-1565 cm^{-1}). Showing the following correlation;

$\nu_{sym.}$ (CC str.) (1565 cm^{-1}) (axial.)(A_{1g}) > $\nu_{asym.}$ (CC str.) (1547 cm^{-1}) (axial.) (A_{2u})

$\nu_{sym.}$ (CC str.) (1565 cm^{-1}) (axial.)(A_{1g}) > $\nu_{asym.}$ (CC str.) (1536 cm^{-1}) (circum.) (E_{1u})

In general:

$\nu_{sym.}$ (CC str.) > $\nu_{asym.}$ (CC str.)

The highest IR absorption intensity is 176.103km/mol due to ν_{94} (1531 cm^{-1}) (A_{2u}).

νRing stretching(CCC stretching vibrations)

Unlike the C--C vibration modes, these are not located at definite C atoms as could be seen from the atomic displacement vectors. According to their assignment, they fall in the range (1108-1507cm^{-1}). The highest IR absorption intensity is 1.660km/mol due to $\nu_{125},_{126}$ (1266 cm^{-1}) (E_{1u}).

δCH in plane CH bending vibrations

Their displacement vectors are mainly located at the corresponding H atoms. The calculated frequency values range is (1126-1466cm^{-1}).

δCH (scissor.) (1466 cm^{-1}) (E_{2u}) > δCH (rock.) (1191cm^{-1}) (E_{1u})

In general:

$\delta CH_{asym.}$ > δCH_{sym}

The highest IR absorption intensity is 0.133km/mol due to $\nu_{127,128}$ (1191 cm^{-1}) (E_{1u}).

δRing in planeCCC bending vibrations (δCCC)

Of smaller values are the deformation (δCCC) vibrations. According to their assignment, they fall in the range (461-1296 cm^{-1}). These modes include the expected clock and anticlockwise vibration motions. There is no δCCC_{sym} for this mode of vibration. The highest IR absorption intensity is 271.985km/mol due to ν_{95} (1296 cm^{-1}) (**A_{2u}**).

γCH out of plane CH bending vibrations

The (γCH) out of plane vibration frequency range is (695-935cm^{-1}).

The following relations hold too;

$\nu_{sym}\gamma$CH (935 cm^{-1}) (wagg.) (A_{1g}) > $\nu_{asym}\gamma$CH (896 cm^{-1}) (twist.) (E_{2u}).

The highest IR absorption intensity is 377.198km/mol due to $\nu_{131, 132}$ (899 cm^{-1}) (E_{1u}).

γCC out of plane (of the molecule) vibrations

The (γCC) out of the plane of the molecule vibration frequency range is (341-765 cm^{-1}).

The highest IR absorption intensity is 17.056km/mol due to $\nu_{133, 134}$ (765 cm^{-1}) (E_{1u}).

γRing out of plane (of the molecule) vibrations (γCCC)

The ring out of plane vibrations (γCCC), show frequency values of which the range is (145-764 cm^{-1}). The modes include puckering, deformations, as well as breathing vibrations of the whole ring. The relation of the symmetric to the asymmetric modes of Zigzag molecule is viewed in the following scheme;

$\nu_{asym.}\gamma$Ring (γCCC) (axial.) (764 cm^{-1}) (E_{1g}) > $\nu_{sym.}\gamma$Ring (γCCC) (axial.) (752 cm^{-1}) (A_{1g})

The highest IR absorption intensity is 286.183km/mol due to ν_{101} (409 cm^{-1}) (A_{2u}).

Compared with the frequencies of Mono ring layer SWCNT [37], as calculated applying the same DFT method and gauss basis, the frequency values and the force field of Mono ring layer are higher for$\nu_{sym.}$CHstr., $\nu_{asym.}$C--Cc str., δCH, δring, γCH wagg., and lower for $\nu_{sym.}$C--Ca str., γCH twist., γring, table-3 , 4. The following relations hold:

$\nu_{sym.}$CH str. Mono > **$\nu_{sym.}$CH str**. Tri
$\nu_{asym.}$CH str. Mono > **$\nu_{asym.}$CH str**. Tri
$\nu_{sym.}$C--Ca str. Tri > **$\nu_{sym.}$C--Ca str.** Mono
$\nu_{asym.}$C--Ca str. Tri > **$\nu_{asym.}$C--Ca str.** Mono
$\nu_{asym.}$C--Cc str. Mono > **$\nu_{asym.}$C--Cc str.** Tri
δCH Mono > **δCH**Tri
δRing(δCCC) Mono > **δRing(δCCC)** Tri
γCH wagg. Mono > **γCH wagg.** Tri
γCH twist. Tri > **γCH twist.** Mono
γRing (γCCC) Tri >γRing (γCCC) Mono

The ordering of the modes follows the Herzberg convention [35]. table-3 includes the calculated vibration frequencies and IR absorption intensities for each mode of the Tri rings layer SWCNT. figure-3 shows the graphical pictures of some vibration modes for Tri-rings layer (6, 0) Zigzag SWCNT as calculated applying the DFT (B3LYP /6-311G) method.

Table 3- Vibration frequencies and IR absorption intensities for Tri-rings layer (6, 0) Zigzag.

	Symmetry & description	PM3	DFT/3-	DFT/6-31G	DFT/6-	DFT/6-
A_{1g}						
ν_1	CHsym. str.	3081	3086	3099	3041	0.000
ν_2	ring (CC str.) (axial) mid layer	1736	1531	1585	1565	0.000
ν_3	ring (CC str.) (axial)	1620	1432	1470	1450	0.000
ν_4	δring (δCCC str.)	1230	1080	1097	1083	0.000
ν_5	γCH (wagging)	921	888	937	935	0.000
ν_6	γring (γCCC) (axial) (puck).	865	715	803	752	0.000
ν_7	γring (γCCC)(puck.) + γCH(breath.)	622	567	613	609	0.000
ν_8	γring (γCCC)(breathing) mid layer	606	492	500	494	0.000
ν_9	γring (γCCC) (puck.) outer edge	437	424	429	431	0.000
ν_{10}	γring (γCCC) (puckering)	389	393	396	394	0.000
A_{2g}						
ν_{11}	δCH (clock-anti clock)	1534	1396	1430	1416	0.000
ν_{12}	CCCstr. (circum.) mid layer + δCH	1282	1284	1341	1318	0.000
ν_{13}	δCH (clock-anti clock)	1098	1163	1190	1175	0.000
ν_{14}	δring (δCCC) (clock-anti clock) + δCH	462	462	464	461	0.000
B_{1g}						
ν_{15}	δCH (scissor.)	1565	1445	1449	1440	0.000
ν_{16}	CCC str. (circum.) mid layer	1543	1354	1382	1362	0.000
ν_{17}	ring str. (CCC str.)	1393	1298	1354	1329	0.000
ν_{18}	δCH (scissor.) + CC str. (axial)	1133	1123	1137	1126	0.000
ν_{19}	γCC (axial) (puckering) + γCH	710	665	690	684	0.000
ν_{20}	γCC (axial) (puckering)	630	665	612	603	0.000
ν_{21}	γCC (axial) (puck.) outer layer	394	348	370	368	0.000
B_{2g}						
ν_{22}	CHasym. str.	3080	3075	3088	3029	0.000
ν_{23}	CCstr. (circum.)	1589	1359	1390	1370	0.000
ν_{24}	CCstr. (circum.)	1566	1263	1294	1269	0.000
ν_{25}	γCH (twisting)	836	852	872	867	0.000
ν_{26}	γCH (twisting)	808	777	797	800	0.000
ν_{27}	γCC (axial) mid layer + γCH	700	656	692	680	0.000
ν_{28}	γCC (axial) mid layer	588	561	577	573	0.000
ν_{29}	γring (γCCC) (puckering)	279	248	266	278	0.000
E_{1g}						
ν_{30}	CHasy. str.	3078	3083	3095	3037	0.000
ν_{32}	CC str. (circum.) + δCH (rock.)	1696	1511	1557	1536	0.000
ν_{34}	CCstr. (axial) outer layer + δCH	1669	1486	1524	1505	0.000
ν_{36}	ring str. + δCH (rock.)	1465	1321	1358	1341	0.000
ν_{38}	CC str. (circum.) + δCH (rock.)	1378	1252	1278	1261	0.000

ν_{40}	δCH (rock.)	1147	1180	1203	1188	0.000
ν_{42}	γCH (twisting)	980	863	885	883	0.000
ν_{44}	γCH(wagg.) +γring (γCCC)(puck.)	904	812	844	837	0.000
ν_{46}	γring (γCCC) (puckering) + γCH	870	752	790	764	0.000
ν_{48}	γring (puckering) mid layer	819	595	773	686	0.000
ν_{50}	γCC (axial) (puckering)	628	673	641	630	0.000
ν_{52}	γCC (axial) (puckering) mid layer	585	608	598	594	0.000
ν_{54}	γCCC (circum.)	352	350	368	369	0.000
ν_{56}	γring (γCCC) (puckering)	304	303	306	304	0.000
E_{2g}						
ν_{58}	CHasy. str.	3079	3078	3090	3032	0.000
ν_{60}	CCCstr. (circum.) + δCH (scissor.)	1667	1496	1523	1507	0.000
ν_{62}	CCstr. (axial)	1595	1374	1421	1397	0.000
ν_{64}	CCstr. (axial) + δCH (scissor.)	1508	1361	1392	1377	0.000
ν_{66}	Ring str. (CCCstr.)	1454	1281	1335	1308	0.000
ν_{68}	δCH (scissor.) + CCCstr. (circum.)	1330	1217	1244	1226	0.000
ν_{70}	Ring str. (CCCstr.)	1192	1104	1124	1108	0.000
ν_{72}	δring(δCCC) mid layer + δCH	1033	910	921	911	0.000
ν_{74}	γCH (twisting)	851	830	868	869	0.000
ν_{76}	γCH (twisting)	795	745	763	759	0.000
ν_{78}	γCH (twist.) +γring (γCCC)(puck.)	676	639	681	673	0.000
ν_{80}	γCC (axial) mid layer (puckering)	504	489	496	495	0.000
ν_{82}	γring (γCCC) (puckering)	458	411	451	453	0.000
ν_{84}	γring (γCCC) (puckering)	247	252	258	259	0.000
ν_{86}	γring (γCCC) (puckering)	148	137	143	145	0.000
A_{1u}						
ν_{88}	ring str. (clock-anti clock.) + δCH	1593	1407	1456	1433	0.000
ν_{89}	δCH (clock-anti clock)	1296	1356	1392	1378	0.000
ν_{90}	δCH (clock-anti clock)	1100	1142	1175	1155	0.000
ν_{91}	δring (δCCC) (clock-anti-clock) (outer	608	601	601	598	0.000
ν_{92}	δring (δCCC) (clock-anti clock) + δCH	252	254	254	253	0.000
A_{2u}						
ν_{93}	CHasy	3081	3085	3099	3041	55.779
ν_{94}	CC str. (axial) outer layer	1700	1504	1551	1531	176.103
ν_{95}	δring (δCCC) (elongation)	1415	1289	1310	1296	271.985
ν_{96}	γCH (wagg.)	930	818	865	867	301.477
ν_{97}	γring (γCCC)	923	774	794	779	128.109
ν_{98}	γring (γCCC) (puckering) outer	897	701	781	729	219.485
ν_{99}	γring (γCCC) (breathing) mid	740	634	745	644	131.016
ν_{100}	γring (γCCC) (breathing)	520	488	500	496	10.266
ν_{101}	γring (γCCC) (puckering) outer	437	398	407	409	286.183
B_{2u}						
ν_{102}	CHasy	3080	3076	3088	3029	0.000
ν_{103}	CCstr. (circum.) outer layer + CCstr.	1576	1344	1372	1351	0.000
ν_{104}	CCstr. mid layer	1562	1311	1368	1344	0.000
ν_{105}	ring str. (CCC str.)	1343	1161	1182	1166	0.000
ν_{106}	γCH (twisting)	821	809	846	846	0.000
ν_{107}	γCH (twisting)	680	691	695	695	0.000
ν_{108}	γCC (axial) mid layer	381	368	390	388	0.000
ν_{109}	γring (γCCC) (puckering)	273	269	285	291	0.000
B_{1u}						
ν_{110}	δCH (scissor.)	1562	1446	1451	1442	0.000
ν_{111}	CCstr. (circum.) + CCstr. (axial)	1519	1296	1351	1326	0.000
ν_{112}	δCH(scissor.) + ring str. (CCC str.)	1337	1284	1313	1291	0.000
ν_{113}	δring (δCCC) + δCH (scissor.)	1077	990	1006	997	0.000
ν_{114}	γCC (axial) (puck.) outer layer	706	650	685	683	0.000
ν_{115}	δring	539	513	523	524	0.000
ν_{116}	γCC (axial)(puckering) outer layer	368	315	340	341	0.000
E_{1u}						
ν_{118}	CHasy	3078	3083	3095	3037	21.440
ν_{120}	CCstr. (axial) + δCH (rock.)	1699	1521	1567	1547	0.065

ν_{122}	CCstr. (axial) mid layer + δCH (rock.)	1601	1418	1458	1440	21.762
ν_{124}	CCstr. (axial)	1568	1390	1433	1412	9.945
ν_{126}	δCH (rock.) + CCCstr. (circum.)	1348	1244	1286	1266	1.660
ν_{128}	δCH (rock.)	1227	1178	1210	1191	0.133
ν_{130}	CCstr. (axial)	886	1049	1068	1054	0.023
ν_{132}	γCH (wagg.)	857	853	899	899	377.198
ν_{134}	γCC (axial) (puck.) outer layer	783	743	792	765	17.056
ν_{136}	γring (γCC) (puckering)	783	672	709	695	1.924
ν_{138}	γring (puckering) + γCH (wagg.)	653	608	709	611	31.955
ν_{140}	γγring (puckering)	498	478	617	522	0.079
ν_{142}	γring (puckering)	408	412	417	416	0.239
ν_{144}	γring (puckering)	257	261	263	263	1.472
E_{2u}						
ν_{146}	CHasy	3079	3078	3090	3032	0.000
ν_{148}	CCCstr. (cercum.) + δCH(scissor.)	1682	1492	1525	1506	0.000
ν_{150}	ring str. + δCH (scissor.)	1617	1458	1482	1466	0.000
ν_{152}	CCstr. outer layer	1546	1320	1377	1350	0.000
ν_{154}	δCH (scissor.) + δring (δCCC)	1427	1270	1285	1272	0.000
ν_{156}	CCCstr. (circum.)	1272	1192	1222	1203	0.000
ν_{158}	δring (δCCC)	1116	1050	1058	1047	0.000
ν_{160}	γCH (twisting)	888	885	900	896	0.000
ν_{162}	γCH (twisting)	845	796	830	831	0.000
ν_{164}	γring (γCC) (axial) (puckering)	809	685	755	709	0.000
ν_{166}	γring (γCC) (axial) outer (puck.)	632	623	635	631	0.000
ν_{168}	γring (γCCC) (axial) (puckering)	613	573	601	594	0.000
ν_{170}	γring (γCCC) (puckering)	505	492	497	495	0.000
ν_{172}	γring (γCC) (axial) (puckering)	363	344	364	364	0.000
ν_{174}	γring (γCCC) (puckering)	163	157	161	163	0.000

γ: Out of plane (of the molecule) bending vibration., δ: In-plane (of the molecule) bending vibration.
Scaling factors: 0.96 (CH str.) for all DFT (B3LYP/6-311G) frequencies, [36].

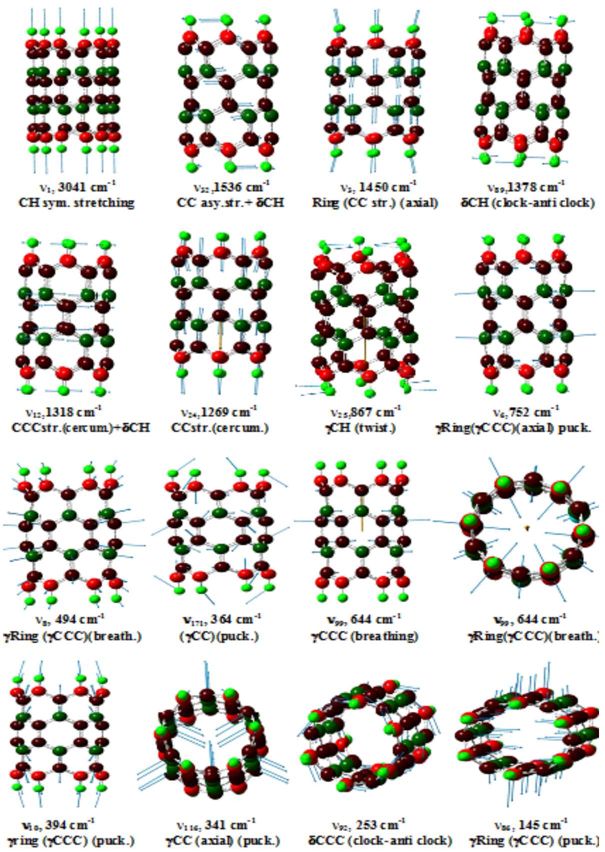

Figure 3- Graphical pictures of some vibration modes for Tri-rings layer (6, 0) Zigzag SWCNT as calculated applying the DFT (B3LYP/6-311G) method.

Table 4-Vibration frequencies for some modes of Mono and Tri-rings layer (6,0) Zigzag SWCNT.

Odd layer	C-H asym	C-H sym.	C--Ca asym	C--Ca sym.	C--Cc asym	δCH sciss	δCH rock.	δring asym	δring sym	γCH wagg asym	γCH wagg sym	γCH twist	γring asym	γring sym
* Mono	3064 A_{2u}	3067 A_{1g}	1516 E_{1u}	1531 A_{1g}	1565 E_{1g}	1274 B_{2g}	1201 A_{1u}	1228 E_{2u}	775 A_{1g}	922 A_{2u}	956 A_{1g}	892 E_{2u}	735 A_{2u}	537 A_{1g}
Tri	3041 A_{2u}	3041 A_{1g}	1547 E_{1u}	1565 A_{1g}	1536 E_{1g}	1466 E_{2u}	1191 E_{1u}	1296A_{2u}	1083 A_{1g}	899 A_{1u}	935 A_{1g}	896 E_{2u}	779 A_{2u}	752 A_{1g}

Calculations of Mulliken electronic charges population analysis by (PM3 and DFT (B3LYP/6-311G) methods, showed, similar to the carbon nanotubes [37-41], the charge densities are mainly concentrated at the circumferential carbon and hydrogen atoms of mono and multi-rings layer SWCNT, parallel with their physical properties for electrical conductivity. The axial carbon atoms are diminishing charges from outer to center **(σC---C outer** > **σC---C mid**. The H atoms are positively charged, the C atoms are of the negative charge, except at carbon atoms of the mid circumference layer, figure-4.

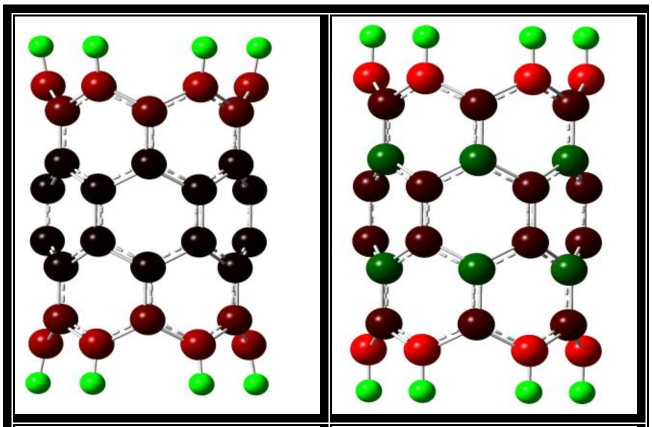

PM3 Tri-rings layer- D_{6h}		DFT Tri-rings layer- D_{6h}	
Electronic charge density		**Electronic charge density**	
—H	**0.114**	**—H**	**0.158**
---C	**-0.062**	**---C**	**-0.133**
---C	**-0.040**	**---C**	**-0.041**
---C	**-0.007**	**---C**	**0.053**
---C	**-0.005**	**---C**	**-0.037**

Figure 4- The Mulliken electronic charges population analysis of Tri rings layer (6,0) Zigzag SWCNT as calculated by PM3 and DFT (6-311G/ B3LYP).

Conclusions:

1-Quantum mechanics semi-empirical PM3 and DFT (3-21G, 6-31G and 6-311G/B3LYP) calculations were carried out for Tri-rings layer of (6,0) Zigzag SWCNT with Gaussian 03 program to investigate the complete vibration frequency modes assignment (3N-6) (IR active and Raman active) at their equilibrium geometries. It showed D_{6h} symmetry point group as well as Mono ring SWCNT.

2-For Tri-rings layer SWCNT (C…Ca) bonds were decrease on going from outer rings layer to mid ring layer, the reverse was shown in the circumferential bonds (C…Cc).

3- Comparison of the geometries, physical properties, vibration frequency modes were done for the two odd SWCNTs. It was shown that ΔH_f, and E_{HOMO}, increase with the increasing number of odd rings layer, E_{LUMO} decrease with the increasing odd rings layer. $\Delta E_{HOMO-LUMO}$ decrease with increasing number of odd rings layer. Dipole moment μ is zero according to their symmetry. The diameter increase with increasing odd rings layer, the diameter of Mono ring layer is lower than the diameter of Tri-rings layers. (C-H) and (C…Ca) bond length in Mono ring layer were shorter than that in Tri rings layer, the reverse was found for (C…Cc) bonds length, which decrease in length with increasing odd rings layers (Tri rings layers),and decrease in length on going from outer to the center of the rings layer (SWCNT)**.**

4-A comparative view of the charge density at the carbon and hydrogen atoms were studied. The calculations show that, the charge densities in both Mono and Tri SWCNTs are mainly concentrated at the hydrogen atoms (positively charged) and at the outer circumferential carbon atoms (negatively charged), and have diminishing charges from outer to the mid of the CNTs.

References

1. Reich S.C., Thomsen C. and Maltzsch J., **2004**. "*Carbon nanotubes basic concepts and physical properties*", Wiley online library.
2. Iijima S., **1991**. "Helical microtubules of graphitic carbon", *Nature* 354 (6348), pp: 56–58.
3. Hamada N., Sawada S. and Oshiyama A., **1992.** "New one-dimensional conductors: graphitic microtubules". *Phys. Rev. Lett*. 68(10), pp: 1579–1581.
4. Wang Y. and Jing X., **2005**. "Intrinsically Conducting Polymers for Electromagnetic Interference Sheilding". *Polym. Adv. Technol*.,16(4), pp: 344-351.
5. Durkop T., Getty S.A., Cobas E. and M.S. **2004**. "Extraordinarymobility in semiconducting carbon nanotubes*". Fuhrer, Nano Lett.* 4(1), pp: 35-39.
6. Yacobson B.I. and Smalley R.E., **1997**. "Fullerene Nanotubes; C1000,000 and Beyond", *American Scientist,* 85, pp: 324-337.
7. Jorio A., Saito R., Hafner J.H., Liebre C.M., Hunter M., Mcclur T. and Dresselhaus G., **2001.** "Structural (n,m)determination of isolated single–wall carbon nanotubes by resonant Raman scattering". *Phys. Rev. Lett* .86 (6), pp: 1118-1121.
8. Dalton A.B., Coleman J.N., McCarthy B., Ajayan P.M., Lefrant S., Bernier P., Blau W. and Byme H.J., **2000**."Selective interaction of semi-conjugated polymer with single wall nanotubes". *J. Phys. Chem*. B. 104(43), pp: 10012-10016.
9. Vitali L., Bughard M., Schneider M.A., LeiLiu Y. Wu., Jayanthi C. andKem K., **2004**. "Phonon spectromicroscopy of carbon nanostructures with atomic resolution", *Max Planck Institute for Solid State Research, Lett.*93(13), pp: 136103-1-136103-4.
10. Kuhlman U., Jantoljak H. , Pfander N., Bernier P., Journet C. and Thomsen C., **1998.** "Infrared active phonons in single-walled carbon nanotubes", *Chem. Phys. Lett.* 294 (1-3), pp: 237-240.
11. Burghard M., **2005**. "Electronic and vibrational properties of chemically modified (SWCNTs)", Surface Science Reports, *Max-plank-Institutfuer, Germany,* 58(4), pp:1-5.
12. Alon O.E., **2001**."Number of Raman and infrared-active vibrations in single-walled carbon nanotubes", *Physical Review* B, 63(20), pp: 201403-1-201403-3.
13. Rao A.M., Richter E., Bandow S.J., Chase B., Eklund P.C., Williams K.A., Fang S., Subbaswamy K.R., Menon M., Thess A., Smalley R. E., Dresselhaus G., Dresselhaus M.S.,**1997**. "Diameter-selective Raman scattering from vibrational modes in carbon nanotubes", *Science*, 275, pp:187-191.
14. Bandow S. and AsakaS. , **1998.** "Effect of the growth temperature on the distribution and chirality of single-wallcarbon nanotubes", *Phys. Rev. Lett*. 80(14), pp: 3779-3782.
15. Popov V.N.and Henrard L, **2002**."Breathing like phonon modes of multiwalled carbon nanotubes", *Phys. Rev. B* 65(23), pp: 235415-235421.
16. Wang C.Y., Ru C.Q., Mioduchowski A., **2005**. "Pressure effect on radial breathing modes of multiwall carbon nanotubes", *J. Appl. Phys*. 97(2),pp: 024310-024310.
17. Li C. Y. and Chou T. W., **2003**.,"Single-walled carbon nanotubes as ultrahigh frequency nanomechanical resonators", *Phys Rev B* 68(7),pp: 073405-073405.
18. Wang Z.L., Poncharal W.A. and de Heer W.A.**, 2000.** "Measuring physical and mechanical properties of individual carbon nanotubes by in situ TEM", *J. Phys. Chem. Solids* 61(7), pp: 1025-1030.

19. Bottani C.E., Bassi A.L., Beghi M.G., Podesta A., Milani P., Zakhidov A., BaughamR.,Walters D.A. and Smalley R.E. **2003**. "Dynamic light scattering from ocoustic modes in single-walled carbon nanotubes", *Phys. Rev. B* 67(15), pp: 155407-155407.

20. Wang C.Y., Zhang Y.Y., Wang C.M., and Tan, V.B.C., **2007**."Buckling of carbon nanotubes", *J. Nanosci.Nanotechno.*7(12), 4221-4247.

21. Gibson R.F., Avorinde E.O. and Wen Y.F., **2007**., "Vibrations of carbon nanotubes and their composites", *Compos. Sci. Technol*. 67(1).1-28

22. Li C.Y. and Chou T.W., 2003., "Vibrational behaviours of multiwalled-carbon-nanotube-based nanomechanical resonators", *Appl. Phys. Lett*. 84(1), 121-124.

23. Wang CY, Ru CQ, Mioduchowski A., **2005**. *"Free vibration of multiwall carbon nanotubes*", *J. Appl. Phys*. 97(11), 114323.

24. Zhou J. and Dong J.M., 2007. "Vibrationl property and Raman spectrum of carbon nanoribbon", *Appl. Phys. Lett*. 91(17), 173108-173111.

25. Xia Y.Y., Zhao M.W., Ma Y.C., Ying M.J., Liu X.D., Liu P.J. and Mei L.M., **2002**. "Tensile strength of single-walled carbon nanotubes with defects under hydrostatic pressure", *Phys. Rev. B* 65 (15), 155415-155421.

26. Jeng Y.R., Tsaia P.C. and Fang T.H. **2004**."Effects of temperature and vacancy defects on tensile deformation of single-walled carbon nanotubes", *J. Phys. Chem. Solid* 65(11), 1849-1856.

27. Scarpa F., Adhikari S. and Wang C.Y., **2009**. "Mechanical properties of non-reconstructed defective single-wall carbon nanotubes", *J. Phys. D-Appl. Phys*. 42(14), 142002-142008.

28. Shen H.S. and Zhang C.L. **2006**."Post buckling prediction of axially loaded double-walled carbon nanotubes with temperature dependent properties and initial defects", *Phys. Rev. B* 74 (3), 035410-035410.

29. Wang C.M., Ma Y.Q., Zhang Y.Y. and Ang K.K., **2006**. "Buckling of double-walled carbon nanotubes modelled by solid shell elements", *J. Appl. Phys*. 99 (11), 114317-114317.

30. Sun C. and Liu K., **2007**. "Vibration of multi-walled carbon nanotubes with initial axial loading", *Solid State Comm*. 143(4-5), 202-207.

31. Bischoff P., **2003**. Molek 9000 Program, OCI, Uni. Heidelerg, Private Communication Pople, J. A.; Gaussian, *Inc. Pittsburgh, PA.*

32. Kubba R.M., Al-AniH.N. and Shanshal M., **2011**."Calculated Vibration Frequencies and IR Absorption Intensities of [6] Cyclacene (zigzag) Molecule", *American Journal of Scientific and Industrial Research, 2(4)*, pp: 642-651.

33. Obot I.B., Obi-Egbedi N.O. and Umoren S.A., **2009.** "Adsorption characteristics and corrosion inhibitive properties of clotrimazole for Aluminium corrosion in hydrochloric acid"**,** *Int. J. Electrochem. Sci.*, 4(6), pp: 863-877.

34. Fleming I.,**1976**. *Frontier Orbitals and Organic Chemical Reactions*, John Wiley and Sons, NewYork.

35. Herzberg G., **1971**. "*Molecular Spectra and Molecular Structure, Infrared and Raman Spectra of Polyatomic Molecules*", Van Nostrand Co. New York.

36. Lewars E., **2004**, "*Computational Chemistry (Introduction to the Theory and Applications of Molecular and Quantum Mechanics)".* Chemistry Department Trent University Peterborough, Ontario, Canada.

37. Kubba R.M., Al-AniH.N. and Shanshal M., **2011.** "The Vibration Frequencies of [6] Cyclacenes (Linear, Angular and Angular-Chiral) Monoring Molecules", *Jordan Journal of Chemistry*, 6(3), pp. 271-293.

38. Krcmar M., Saslow W.M. and Zangwill A.,**2003**. "Electrostatic of Conducting Nanocylinder", *J. Appl. phys.*93(6), pp. 3495-3500.

39. Odom T. W., Huang J., Kim P. and Lieber C. M., **2000**. "Structure and Electronic Properties of CNT", *J. Phy. Chem.,*104(13), pp: 2794-2809.

40. Han S. and Hrm J.I., **2000**. "Role of the localized states in field emission of carbon nanotubes", *Phys. Rev*. B 61(15), pp: 9986-9989.

41. Li C.Y. and Chou T.W. **2007**. "Continuum percolation of nanocomposites with fillers of arbitrary", *Appl. Phys. Lett.*, 90 (17), pp: 174108-174111.